Ephaptic Coupling as a Resolution to the Paradox of Action Potential Wave Speed and Discordant Alternans Spatial Scales in the Heart

Niels F. Otani,[1,*] Eileen Figueroa,[1] James Garrison,[2] Michelle Hewson,[3] Laura Muñoz,[1] Flavio H. Fenton,[4] Alain Karma,[5] and Seth H. Weinberg[6]

[1]*Rochester Institute of Technology, Rochester, New York 14623, USA*
[2]*Hampden-Sydney College, Hampden-Sydney, Virginia 23943, USA*
[3]*Western Carolina University, Cullowhee, North Carolina 28723, USA*
[4]*Georgia Institute of Technology, Atlanta, Georgia 30332, USA*
[5]*Northeastern University, Boston, Massachusetts 02115, USA*
[6]*The Ohio State University, Columbus, Ohio 43210, USA*

(Received 19 October 2022; accepted 7 March 2023; published 23 May 2023)

Previous computer simulations have suggested that existing models of action potential wave propagation in the heart are not consistent with observed wave propagation behavior. Specifically, computer models cannot simultaneously reproduce the rapid wave speeds and small spatial scales of discordant alternans patterns measured experimentally in the same simulation. The discrepancy is important, because discordant alternans can be a key precursor to the development of abnormal and dangerous rapid rhythms in the heart. In this Letter, we show that this paradox can be resolved by allowing so-called ephaptic coupling to play a primary role in wave front propagation in place of conventional gap-junction coupling. With this modification, physiological wave speeds and small discordant alternans spatial scales both occur with gap-junction resistance values that are more in line with those observed in experiments. Our theory thus also provides support to the hypothesis that ephaptic coupling plays an important role in normal wave propagation.

DOI: 10.1103/PhysRevLett.130.218401

Introduction.—Ventricular fibrillation is a dangerous and lethal rhythm disorder of the heart, which can be caused by a spatiotemporal phenomenon called "discordant alternans" [1–6]. Electrical alternans is a complex, emergent, spatiotemporal pattern of electrical waves in the heart whose morphology alternates from one beat to the next and generally arises during fast heart rates or short basic cycle lengths (BCLs) [7,8]. In discordant alternans, this temporal alternating pattern in the action potential duration (APD) develops spatially into regions that are out of phase with one another [1]. As a result, large APD gradients can form in space, which provides a substrate susceptible to the formation of cardiac arrhythmias. However, computer models of discordant alternans using the standard cable equation tend to yield out-of-phase regions, or "domains," too large to fit within the heart (i.e., several centimeters in size, in particular in the presence of physiologically realistic conduction velocities) [2,9–13], whereas in experiments, domains have been shown to occur with much smaller sizes (i.e., on the order of 1 cm or smaller) [6,13–20].

We hypothesize that this apparent noted experimental-computational discrepancy [17] is related to differences in the value of gap-junction resistance. Experimental measurements have found a wide range of values for the gap-junction resistance, typically in the tens to hundreds of megohms (a few to low hundreds of nanosiemens) [21–32]; yet common values for resistances used in simulations employing physical units are 1–2 orders of magnitude lower [33–39]. Simulation studies representing cardiac tissue as a continuous spatial domain via the cable equation include cell-cell coupling through the use of a diffusion coefficient. Here too, the values of the coefficient typically used (on the order of 0.001 cm^2/ms) correspond to gap-junction resistances much lower than experimental measurements. In both cases, lower gap-junction resistance or higher diffusion coefficient values are generally chosen in simulations to match experimental observations of the action potential wave speed, typically at least in the 50–60 cm/s range. However, these same values result in smaller APD gradients in simulations [40] and thus larger spatial domains during discordant alternans [2,9–13]. As a result, simulations using standard models of cell-cell coupling that employ gap-junction resistance values that permit realistic wave propagation speeds are generally unable to produce discordant alternans domains of realistic size (∼1 cm). This is the fundamental paradox we address in this study: how can both fast conduction velocity and the steep repolarization gradients apparently necessary for small domains be maintained at the same time in the same tissue?

We emphasize that this paradox reflects fundamental inconsistencies with our current understanding of the

interaction between cell-cell coupling, wave propagation, and alternans pattern formation. We posit that the paradox is resolved by accounting for an additional cell-cell coupling mechanism, so-called "ephaptic" coupling, as previously described by several previous studies [33,41–53]. Ephaptic coupling requires a high density of sodium channels clustered at the cell-cell junctions. When mediated by ephaptic coupling, wave front propagation occurs through the activation of sodium channels in the upstream or prejunctional cell, which produces a fast inward current that hyperpolarizes the narrow cleft space between coupled cells. Sufficient hyperpolarization can activate sodium channels on the downstream or postjunctional cell.

Many prior studies, including our own, have demonstrated that ephaptic coupling can strongly influence cardiac conduction, depending on key structural properties such as the width of the intercellular cleft space and the fraction of sodium channels near the cleft, in addition to the gap-junction resistance [33,42,46,47,50,53,54]. Indeed, near-normal action potential wave propagation speeds are still possible through ephaptic coupling using realistic gap-junction resistances, as has been demonstrated by Kucera *et al.* [33].

In contrast, no prior studies have addressed how both ephaptic and gap-junctional coupling impact the spatial gradients that arise during the rapid rates that produce alternans. We observe that, on the trailing edge of the action potential, sodium channels are inactive under normal conditions, so that coupling between cells is solely mediated by gap junctions, irrespective of whether wave front dynamics is mediated by gap-junction or ephaptic dynamics. Thus, when ephaptic effects are important, the dynamics of the propagating action potential differ on the leading and trailing edges of the wave. This "decoupling" between the mechanisms governing wave front and wave back dynamics provides the basis for our main hypothesis—that high gap-junction resistance and the strong ephaptic effects created by optimal cleft spacing and a high cell-cell junctional sodium channel density can support the simultaneous presence of rapid waves and small discordant alternans domain sizes. That is, both ephaptic and gap-junction coupling facilitate rapid wave front propagation, while, at the same time, high gap-junction resistance reduces cell-cell coupling on the wave back, allowing steep APD spatial gradients and the development of small discordant alternans domains.

Methods.—To test our hypothesis, we constructed a computer model of a one-dimensional fiber that employs a simplified version of an electric circuit previously used by Kucera *et al.* [33] and us [42–45,51,55] to model gap-junction and ephaptic coupling (Fig. 1). To calculate the values of electrical components, we considered the cells to be cylindrical, with radius $r = 11$ μm and length $\Delta x = 100$ μm, arranged end to end to form the fiber. A narrow space, typically referred to as the cleft region, of width w_{cl}, separated the cells. Values of the resistors R_i and R_r and capacitors C_{cl} and C_m were computed assuming this geometry; the generic formulas $R = \rho L/A$ and $C = c_m A$ were used, where A and L are the appropriate cross-sectional area and length, respectively, through which current flows, $c_m = 1.0\ \mu\mathrm{F/cm^2}$ is the membrane capacitance per unit area, and a resistivity $\rho = 150\ \Omega\,\mathrm{cm}$ was assumed for both the intracellular and cleft spaces. The gap-junction resistance R_g varied from 3.95 to 395 MΩ, corresponding to gap-junction conductances from 253 down to 2.53 nS. The nonlinear current sources I_m and I_{cl} were derived from the ionic currents in the three-variable Echebarria and Karma model [56], scaled appropriately given our geometry and an assumed membrane potential range between −85 mV (resting state) and +15 mV (fully activated state). Conductances were scaled to represent the high density of sodium channels on the cleft-facing junction membranes relative to the overall density of sodium channels [33,42,54]. Minor parameter modifications were made to yield typical APDs of ∼200 ms and conduction velocities of 50–60 cm/s for the gap-junction-dominated case. Equations were advanced in time using the backward Euler method for the passive linear components (the resistors and capacitors) and the forward Euler method for the nonlinear components, with a time step of 0.01 ms. The system consisted of 320 cells, yielding a system length of 3.2 cm. Additional details appear in the companion paper [57].

Results.—For purposes of comparison, we first ran our simulation with parameters known to facilitate wave propagation via standard gap-junction coupling, which

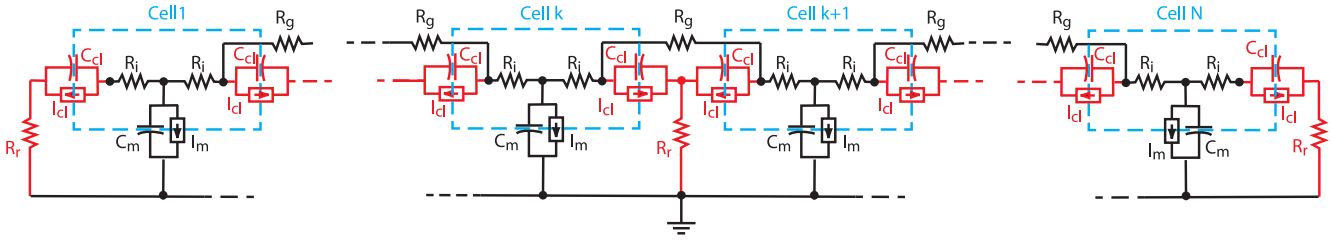

FIG. 1. Circuit used to model a one-dimensional fiber containing gap-junction and ephaptic intercellular coupling. Black circuit elements are those typically used in standard, monodomain models of one-dimensional fibers. Red elements model ephaptic coupling. Blue dashed boxes indicate the locations of cells within this circuit description of the fiber.

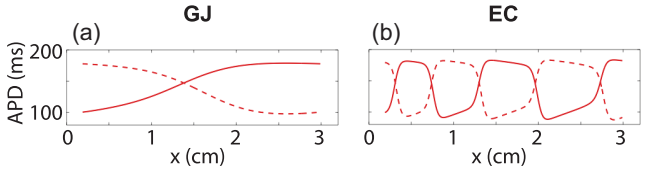

FIG. 2. APD(x) vs x for two consecutive waves (solid and dashed curves), showing transition(s) from long-short to short-long APDs in space for both the (a) GJ and (b) EC systems during regular pacing, with all waves being launched at the left end of the system. Data are shown approximately 120 s into the simulation, well after initial transient behavior has disappeared. Pacing interval (BCL), 207 ms.

we will refer to as the GJ system. Specifically, with a relatively low gap-junction resistance R_g of 3.95 MΩ, a fast inward conductance τ_{fi}^{-1} of 3.0 ms^{-1}, a cleft width w_{cl} of 26 nm, and uniform distribution of fast inward ion channels over the surface of the cells, we obtained a maximum wave velocity of 56.7 cm/s. (In this model, τ_{fi}^{-1} plays the role of the conductance associated with the fast inward current, where τ_{fi} is commensurate with the action potential wave front rise time.) When this model was subjected to rapid pacing (cycle length of 207 ms) on one end of the fiber (at $x = 0$), it produced, as expected, the same long length scale pattern of discordant alternans [Fig. 2(a)] others have seen when wave propagation was mediated by standard gap-junction coupling [2,9–13]. This pattern shows portions of two discordant alternans domains (i.e., regions in which the long-short-long-short patterns of APDs or DIs (diastolic intervals) are in phase), separated by a gradual transition region close to 1.0 cm wide.

Next, we performed a large number of simulations characterized by wave propagation that is mediated primarily by ephaptic coupling. Many prior studies have shown that ephaptic coupling requires high cleft-localized surface density of fast inward sodium current [33,42,47,50], which is supported by imaging studies of sodium channel localization [33,54,58]. Therefore, ephaptic coupling was implemented by redistributing 90% of the fast inward channels to the ends of the cells, while keeping constant the total number of these channels. Further, we increased the gap-junction resistances 100-fold ($R_g = 395$ MΩ), to values more in line with those typically observed in experiment [21–32]. Several values of the cleft width w_{cl} ranging between 12 and 26 nm, and fast inward conductivities τ_{fi}^{-1} varying between 3.75 and 5.00 ms^{-1}, were used. Consistent with earlier studies, we found wave speeds comparable to the gap-junction-dominated case: 48–70 cm/s. (See the companion paper for additional details [57].)

Results from the system with $\tau_{\mathrm{fi}}^{1} = 3.75$ ms^{-1} and $w_{\mathrm{cl}} = 26$ nm, which we call the EC system, are representative of these simulations. (Some simulations exhibited a minor variation from the behavior exhibited by the EC system; these are described in the companion paper [57].) As shown in Fig. 2(b), the pattern of discordant alternans is strikingly different in two ways: First, the size of the discordant alternans domains is considerably smaller, approximately 0.6 cm in width, compared to nearly 3 cm for the GJ case shown in Fig. 2(a). Second, the transition regions between domains (called "nodes") are quite sharp, resulting in a spatial pattern with a steeper APD gradient, which has also been seen experimentally [1,17–19]. This pattern persisted over the entire range of cycle lengths for which APD alternans was present (201–215 ms). As shown in Fig. 3(a), the domain sizes for the EC system were less than 0.8 cm over this entire range and decreased to near 0.1 cm for the shortest cycle lengths. In contrast, in the GJ system, domain sizes were between 2.4 and 3 cm, generally decreasing as cycle length shortened. Also, as shown in Fig. 3(d), the nodal widths were much smaller for the EC system (0.1–0.25 cm) compared to the GJ system (0.9–1.5 cm). These striking differences were obtained despite the GJ and EC systems having virtually identical APD restitution functions and very similar conduction velocity restitution functions, with, in particular, both systems having nearly identical maximum wave propagation speeds (~56 cm/s).

We hypothesize that these large differences in the discordant alternans pattern are due to the larger gap-junction resistances present in the ephaptic simulations, which permit the APD for a given wave to vary over much shorter distances than is possible in the gap-junction-dominated systems. To investigate this possibility, we followed the approach of Echebarria and Karma [59], by assuming that the APD along the fiber for a given wave is governed by the equation,

$$\mathrm{APD}(x) = a[\mathrm{DI}(x)] - w\frac{d}{dx}a[\mathrm{DI}(x)] + \xi^2\frac{d^2}{dx^2}a[\mathrm{DI}(x)], \tag{1}$$

where $a(\mathrm{DI})$ is the APD restitution function obtained in the absence of all cell-cell coupling, ξ represents the characteristic length scale over which the APD can respond to spatial variations in DI, and the $w(da/dx)$ term is an adjustment due to the breaking of $\pm x$ symmetry caused by the directionality and finite speed of wave propagation. Additional details appear in [59].

We explored this hypothesized relationship by collecting the following simulation data: $\mathrm{APD}(x)$, $d\mathrm{APD}(x)/dx$, $d^2\mathrm{APD}(x)/dx^2$, and $\mathrm{DI}(x)$, and then performing nonlinear multiple regression on Eq. (1) with $a(\mathrm{DI})$ taking the standard form, $a(\mathrm{DI}) = \beta_1 - \beta_2\exp(-\mathrm{DI}/\beta_3)$. The regression technique yielded best-fit values for ξ, w, β_1, β_2, and β_3. Our main interest was the value of ξ, which is plotted vs cycle length for the two systems in Fig. 3(c). We observe that the length scale ξ is smaller by a factor of 10 for the EC system, compared with GJ, demonstrating that the APD coupling is much weaker in the ephaptic system.

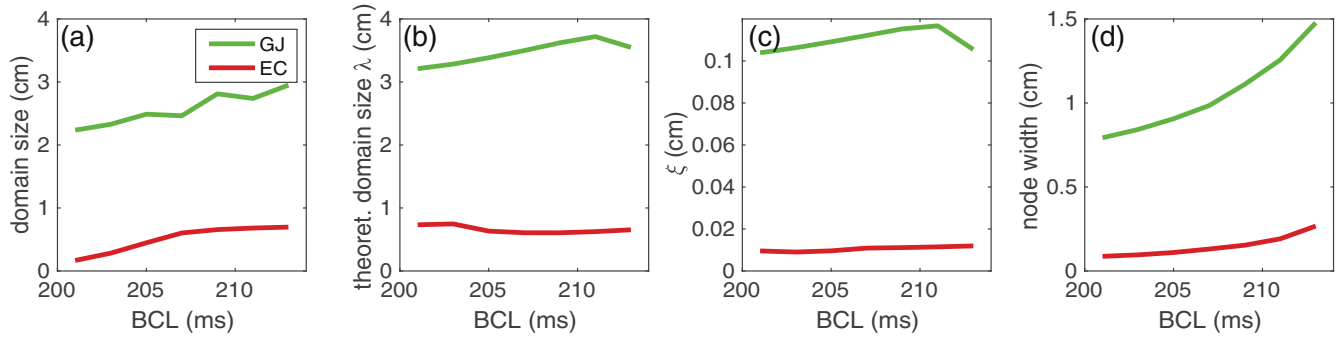

FIG. 3. Key discordant alternans parameters: (a) simulation domain size, (b) theoretical domain size λ, (c) ξ and (d) simulation nodal width, all vs pacing cycle length.

From the data, we were able to put an upper bound on the absolute value of the parameter w—upon doing so, we found that $|w|^3 \ll \xi^4/\Lambda$, which, according to Echebarria and Karma [60], defines the system as operating in the dispersive regime. Here, $\Lambda = [c(\mathrm{DI})]^2/[2c'(\mathrm{DI})]$ was evaluated at the bifurcation point, which we obtained from the conduction velocity restitution function $c(\mathrm{DI})$ from a separate nonlinear regression calculation using the simulation data. In this regime, the discordant alternans domain size can be calculated as $\lambda = (2\pi/\sqrt{3})(2\xi^2\Lambda)^{1/3}$. The values of λ we obtained for both the GJ and EC systems for the range of cycle lengths exhibiting alternans is shown in Fig. 3(b). Note that, while the formula is not strictly applicable to our simulations, as alternans amplitudes are too large to be considered in the linear regime and the range of cycle lengths departs significantly from the bifurcation point at BCL $\approx$ 216 ms (both assumptions of the theory), we found that theoretical values agreed favorably with the domain sizes obtained from the simulation [cf. Figs. 3(a) and 3(b)].

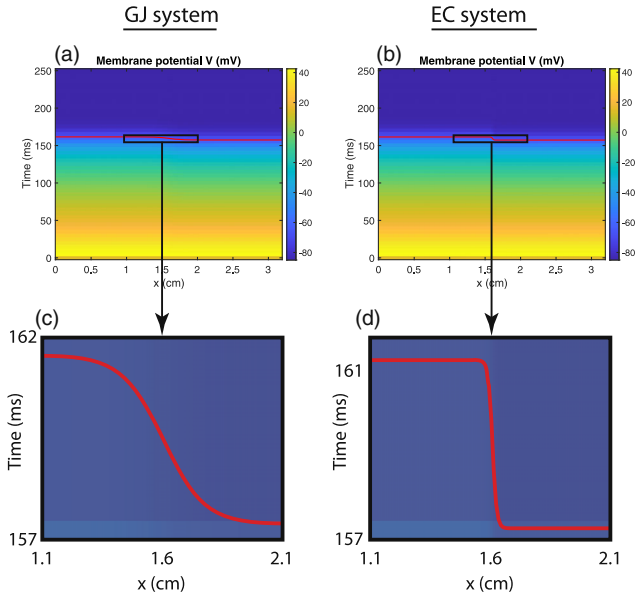

FIG. 4. Color plots of V_m of a single action potential excited simultaneously at all points on the fiber, but with slightly different initial conditions in each half of the fiber: $h = 0.55$ and $f = 0.82$ for $x \leq 1.6$ cm, and $h = 0.50$ and $f = 0.80$ for $x > 1.6$ cm, for (a) the GJ system and (b) the EC system. (c),(d) Enlargement of the location of the wave back for the conditions in (a),(b).

Finally, we demonstrated directly that the APD coupling in the EC systems was much weaker than the GJ system. To do this, we simulated the GJ and EC systems with slightly different gating variable initial conditions on each half of the fiber, with an abrupt transition between the two halves, at $x = 1.6$ cm. We then eliminated any directionality effect by activating the entire fiber simultaneously by raising the membrane potential V_m to $+15$ mV in all cells at $t = 0$ (Fig. 4). As shown in Figs. 4(a) and 4(b), the end of the action potential was essentially constant in each half of each fiber, except in the vicinity of the boundary between the two halves. In an enlargement of this transition [Figs. 4(c) and 4(d)], we see that the EC system exhibits a membrane potential gradient that is much sharper than the one appearing in the GJ system.

Discussion.—In this study, we have demonstrated that, despite having APD and conduction velocity restitution functions that are nearly identical to the gap-junction system, the ephaptic-coupling-dominated systems were characterized by a number of measures that were much smaller, from a minimum of 4 times smaller near the alternans bifurcation point (BCL = 215 ms), up to 10–16 at the shortest cycle lengths (BCL = 203 ms). These measures included (1) the length scale ξ, which is a measure of the dependence of APD in a given cell on APDs in neighboring cells, (2) the domain sizes predicted by theory based on the value of ξ, (3) the actual domain sizes observed in simulations, (4) the width of the nodes, i.e., the transition region between domains, and (5) the width of the transition region when APD (as predicted by the APD restitution function) changes abruptly in space (Fig. 4).

These observations from the simulations are strongly suggestive of a strong connection existing between the weakness of APD coupling and small domain size, and of an independence of these effects from wave front

dynamics. Thus, the observations are not consistent with gap-junction-dominated wave propagation, since, in that case, gap-junction coupling simultaneously governs both wave propagation speed and APD coupling, effectively forcing both to vary together. In contrast, the observations are consistent with ephaptic effects being important and indeed necessary, because different coupling mechanisms exist on the wave front and wave back of propagating waves. Specifically, wave front dynamics and propagation speeds may be dictated by ephaptic effects (in addition to gap-junction coupling), while wave back dynamics and the coupling of the APDs of neighboring cells are dominated by only gap junctions, since sodium current, which typically mediates ephaptic coupling, is absent on the wave back. It is this independence between wave front and wave back mechanisms that allows small domain size to exist even in the presence of rapid wave front speeds. Further, we note that, while the specific range of cycle lengths for which the discordant alternans patterns form will differ across models, species, and conditions, this mechanism of wave front and wave back independence is a tissue-scale coupling phenomenon and does not depend on the underlying cellular instability driving alternans formation; thus we hypothesize this mechanism is broadly applicable and generalizes to all cardiac tissue.

We note that the weak APD coupling in our ephaptic-mediated simulations is not due directly to the ephaptic coupling, but rather to the fact that we raised the gap-junction resistance by a factor of 100 compared to the gap-junction-dominated cases, while still maintaining physiologically realistic wave propagation speeds (50–60 cm/s). It is this gap-junction resistance increase that weakens APD coupling and allows small spatial features, such as small discordant alternans domains and steep voltage gradients. Far from being artificial, this increase in gap-junction resistance is actually an improvement in the model, as these larger resistances (3.95–395 MΩ, up from 395 kΩ) are more in line with resistances measured experimentally [21–31]. Indeed, the resistances used in standard gap-junction coupled models have typically been artificially chosen too low relative to experimental values, in order to reproduce the wave propagation speeds typically observed physiologically.

Our study suggests that ephaptic coupling effects may be important when small-scale (i.e., less than 1 cm) discordant alternans domains are present. It also provides support to the idea that ephaptic effects may be important for wave propagation more generally. It may be the case that gap-junction resistance is normally low, but is high in pathological cases, leading to the formation, or the possibility of formation, of short-wavelength discordant alternans patterns. Alternatively, with most experimental evidence pointing to high values for the gap-junction resistance, there exists the possibility that normal propagation is always mediated by ephaptic coupling. More broadly, our study also suggests that ephaptic coupling may be relevant to repolarization gradients due to intrinsic regional heterogeneity, such as in transmural or apico-basal differences, which would be more strongly expressed when gap-junction resistance is high.

Further research will hopefully resolve these questions, which is important for our understanding and modeling of both action potential wave propagation and the nature of discordant alternans. Critically, both propagation and discordant alternans patterns are key factors in the initialization of rapid cardiac rhythm disorders [5]. Prior experimental studies have shown that modulating either ephaptic or gap-junction coupling can promote arrhythmia incidence [54,61]. A rigorous understanding of the role of, and interactions between, ephaptic and gap-junction coupling in arrhythmia formation requires extending these studies to two- and three-dimensional tissues. Further, it may be critical to incorporate additional tissue structural factors, such as anisotropy and heterogeneity, and the voltage-dependent gating of gap junctions in such a study of arrhythmias. Recent studies have predicted that dynamical gap-junction gating minimally impacts propagation for conditions supporting fast conduction (as in the current study), but can alter predictions of heterogeneous and slow conduction present during arrhythmias [42,62,63]. Further study of the role of the relative distribution of sodium channels on the cell ends vs lateral membrane, which could impact anisotropy as well, is necessary. Such investigations will be a focus of our future work.

We gratefully acknowledge the National Science Foundation's Research Experience for Undergraduates Program Principal Investigator, Darren Narayan (N. F. O., L. M.) Grant No. DMS-1950189, which supported J. G. and M. H., and the NSF Louis Stokes Alliance for Minority Participation Program and the RIT Ronald E. McNair Post-Baccalaureate Achievement Program, which jointly supported E. F. This project was conceived at the Kavli Institute for Theoretical Physics, at the Integrative Cardiac Dynamics Workshop, Summer, 2018 (N. F. O., A. K., S. H. W., L. M., F. H. F.), NSF Grant No. PHY-1748958. This study was supported by funding from National Institutes of Health Grants No. R01HL138003 (S. H. W.), No. R15HL147348 (N. F. O., F. H. F.), and No. R01HL143450 (F. H. F.).

*nfosma@rit.edu

[1] J. M. Pastore, S. D. Girouard, K. R. Laurita, F. G. Akar, and D. S. Rosenbaum, Circulation **99**, 1385 (1999).
[2] M. A. Watanabe, F. H. Fenton, S. J. Evans, H. M. Hastings, and A. Karma, J. Cardiovasc. Electrophysiol. **12**, 196 (2001).
[3] Z. Qu, A. Garfinkel, P.-S. Chen, and J. N. Weiss, Circulation **102**, 1664 (2000).
[4] J. J. Fox, M. L. Riccio, F. Hua, E. Bodenschatz, and R. F. Gilmour, Jr., Circ. Res. **90**, 289 (2002).

[5] B.-R. Choi, W. Jang, and G. Salama, Heart Rhythm **4**, 1057 (2007).
[6] A. Gizzi, E. Cherry, R. F. Gilmour Jr, S. Luther, S. Filippi, and F. H. Fenton, Front. Physiol. **4**, 71 (2013).
[7] M. R. Guevara, G. Ward, A. Shrier, and L. Glass, IEEE Comp. Cardiol. **562**, 167 (1984).
[8] J. Nolasco and R. W. Dahlen, J. Appl. Physiol. **25**, 191 (1968).
[9] E. M. Cherry and F. H. Fenton, Am. J. Physiol. **286**, H2332 (2004).
[10] D. Sato, Y. Shiferaw, A. Garfinkel, J. N. Weiss, Z. Qu, and A. Karma, Circ. Res. **99**, 520 (2006).
[11] D. Sato, D. M. Bers, and Y. Shiferaw, PLoS One **8**, e85365 (2013).
[12] C. Huang, Z. Song, J. Landaw, and Z. Qu, Biophys. J. **118**, 2574 (2020).
[13] H. Hayashi, Y. Shiferaw, D. Sato, M. Nihei, S.-F. Lin, P.-S. Chen, A. Garfinkel, J. N. Weiss, and Z. Qu, Biophys. J. **92**, 448 (2007).
[14] S. Mironov, J. Jalife, and E. G. Tolkacheva, Circulation **118**, 17 (2008).
[15] C. De Diego, R. K. Pai, A. S. Dave, A. Lynch, M. Thu, F. Chen, L.-H. Xie, J. N. Weiss, and M. Valderrábano, Am. J. Physiol. **294**, H1417 (2008).
[16] Y.-C. Hsieh, J.-C. Lin, C.-Y. Hung, C.-H. Li, S.-F. Lin, H.-I. Yeh, J.-L. Huang, C.-P. Lo, K. Haugan, B. D. Larsen *et al.*, Heart Rhythm **13**, 251 (2016).
[17] I. Uzelac, Y. C. Ji, D. Hornung, J. Schröder-Scheteling, S. Luther, R. A. Gray, E. M. Cherry, and F. H. Fenton, Front. Physiol. **8**, 819 (2017).
[18] K. Kulkarni, R. Visweswaran, X. Zhao, and E. G. Tolkacheva, Biomed Res. Int. **2015**, 170768 (2015).
[19] I. Uzelac, A. Kaboudian, S. Iravanian, J. G. Siles-Paredes, J. C. Gumbart, H. Ashikaga, N. Bhatia, R. F. Gilmour Jr, E. M. Cherry, and F. H. Fenton, Heart Rhythm O2 **2**, 394 (2021).
[20] D. J. Christini, M. L. Riccio, C. A. Culianu, J. J. Fox, A. Karma, and R. F. Gilmour Jr., Phys. Rev. Lett. **96**, 104101 (2006).
[21] T. Desplantez, E. Dupont, N. J. Severs, and R. Weingart, J. Membr. Biol. **218**, 13 (2007).
[22] B. R. Kwak and H. J. Jongsma, Mol. Cell. Biochem. **157**, 93 (1996).
[23] M. L. McCain, T. Desplantez, N. A. Geisse, B. Rothen-Rutishauser, H. Oberer, K. K. Parker, and A. G. Kleber, Am. J. Physiol. **302**, H443 (2012).
[24] A. Moreno, M. Rook, G. Fishman, and D. Spray, Biophys. J. **67**, 113 (1994).
[25] V. Valiunas, E. C. Beyer, and P. R. Brink, Circ. Res. **91**, 104 (2002).
[26] S. Verheule, M. J. Van Kempen, P. H. t. Welscher, B. R. Kwak, and H. J. Jongsma, Circ. Res. **80**, 673 (1997).
[27] R. White, J. Doeller, V. Verselis, and B. Wittenberg, J. Gen. Physiol. **95**, 1061 (1990).
[28] M. S. Nielsen, L. Nygaard Axelsen, P. L. Sorgen, V. Verma, M. Delmar, and N.-H. Holstein-Rathlou, Compr. Physiol. **2**, 1981 (2012).
[29] A. Rüdisüli and R. Weingart, Pflügers Arch. **415**, 12 (1989).
[30] R. Weingart, J. Physiol. **370**, 267 (1986).
[31] B. A. Wittenberg, R. White, R. D. Ginzberg, and D. C. Spray, Circ. Res. **59**, 143 (1986).
[32] R. S. Kieval, J. F. Spear, and E. Moore, Circ. Res. **71**, 127 (1992).
[33] J. P. Kucera, S. Rohr, and Y. Rudy, Circ. Res. **91**, 1176 (2002).
[34] R. M. Shaw and Y. Rudy, Circ. Res. **81**, 727 (1997).
[35] M. S. Spach, J. F. Heidlage, P. C. Dolber, and R. C. Barr, Circ. Res. **86**, 302 (2000).
[36] Y. Wang and Y. Rudy, Am. J. Physiol. **278**, H1019 (2000).
[37] Y. Xie, D. Sato, A. Garfinkel, Z. Qu, and J. N. Weiss, Biophys. J. **99**, 1408 (2010).
[38] B. Muller-Borer, D. Erdman, and J. Buchanan, IEEE Trans. Biomed. Eng. **41**, 445 (1994).
[39] Y. Xie, A. Garfinkel, P. Camelliti, P. Kohl, J. N. Weiss, and Z. Qu, Heart Rhythm **6**, 1641 (2009).
[40] K. J. Sampson and C. S. Henriquez, Am. J. Physiol. **289**, H350 (2005).
[41] N. Wei, Y. Mori, and E. G. Tolkacheva, J. Theor. Biol. **397**, 103 (2016).
[42] S. Weinberg, Chaos **27**, 093908 (2017).
[43] M. B. Nowak, A. Greer-Short, X. Wan, X. Wu, I. Deschênes, S. H. Weinberg, and S. Poelzing, Biophys. J. **118**, 2829 (2020).
[44] M. B. Nowak, R. Veeraraghavan, S. Poelzing, and S. H. Weinberg, Front. Physiol. **12**, 1843 (2021).
[45] M. B. Nowak, S. Poelzing, and S. H. Weinberg, J. Mol. Cell. Cardiol. **153**, 60 (2021).
[46] J. Lin and J. P. Keener, Proc. Natl. Acad. Sci. U.S.A. **107**, 20935 (2010).
[47] J. Lin and J. P. Keener, IEEE Trans. Biomed. Eng. **60**, 576 (2013).
[48] J. Lin and J. P. Keener, Biophys. J. **106**, 925 (2014).
[49] N. Moise, H. Struckman, C. Dagher, R. Veeraraghavan, and S. Weinberg, J. Gen. Physiol. **153**, e202112897 (2021).
[50] Y. Mori, G. I. Fishman, and C. S. Peskin, Proc. Natl. Acad. Sci. U.S.A. **105**, 6463 (2008).
[51] A. Greer-Short, S. A. George, S. Poelzing, and S. H. Weinberg, Circulation **10**, e004400 (2017).
[52] E. Ivanovic and J. P. Kucera, J. Physiol. **599**, 4779 (2021).
[53] E. Hichri, H. Abriel, and J. P. Kucera, J. Physiol. **596**, 563 (2018).
[54] R. Veeraraghavan, J. Lin, G. S. Hoeker, J. P. Keener, R. G. Gourdie, and S. Poelzing, Pflügers Arch. **467**, 2093 (2015).
[55] K. Y. Joseph, J. A. Liang, S. H. Weinberg, and N. A. Trayanova, J. Mol. Cell. Cardiol. **162**, 97 (2022).
[56] B. Echebarria and A. Karma, Eur. Phys. J. **146**, 217 (2007).
[57] N. F. Otani, E. Figueroa, J. Garrison, M. Hewson, L. Munoz, F. H. Fenton, A. Karma, and S. H. Weinberg, companion paper, Phys. Rev. E **107**, 054407 (2023).
[58] R. Veeraraghavan and R. G. Gourdie, Mol. Biol. Cell **27**, 3583 (2016).
[59] B. Echebarria and A. Karma, Phys. Rev. E **76**, 051911 (2007).
[60] B. Echebarria and A. Karma, Phys. Rev. Lett. **88**, 208101 (2002).
[61] R. Veeraraghavan, J. Lin, J. P. Keener, R. Gourdie, and S. Poelzing, Pflügers Arch. **468**, 1651 (2016).
[62] D. E. Hurtado, J. Jilberto, and G. Panasenko, PLoS Comput. Biol. **16**, e1007232 (2020).
[63] A. Saliani, S. Biswas, and V. Jacquemet, Chaos **32**, 043113 (2022).